

Nanostructured Biocomposite Scaffolds Based on Collagen Coelectrospun with Nanohydroxyapatite

Vinoy Thomas,^{†,‡,§} Derrick R. Dean,^{*,‡} Moncy V. Jose,^{†,‡} Bini Mathew,[‡] S. Chowdhury,[†] and Yogesh K. Vohra[†]

Center for Nanoscale Materials and Biointegration (CNMB), Department of Physics, University of Alabama at Birmingham (UAB), Alabama 35294, and Department of Materials Science and Engineering, University of Alabama at Birmingham (UAB), Birmingham, Alabama 35216

Received September 15, 2006; Revised Manuscript Received November 19, 2006

Nanofibrous biocomposite scaffolds of type I collagen and nanohydroxyapatite (nanoHA) of varying compositions (wt %) were prepared by electrostatic cospinning. The scaffolds were characterized for structure and morphology by Fourier transform infrared spectroscopy (FT-IR), scanning electron microscopy (SEM), atomic force microscopy (AFM) and X-ray diffraction (XRD) techniques. The scaffolds have a porous nanofibrous morphology with random fibers in the range of 500–700 nm diameters, depending on the composition. FT-IR and XRD showed the presence of nanoHA in the fibers. The surface roughness and diameter of the fibers increased with the presence of nanoHA in biocomposite fiber as evident from AFM images. Tensile testing and nanoindentation were used for the mechanical characterization. The pure collagen fibrous matrix (without nanoHA) showed a tensile strength of 1.68 ± 0.10 MPa and a modulus of 6.21 ± 0.8 MPa with a strain to failure value of $55 \pm 10\%$. As the nanoHA content in the randomly oriented collagen nanofibers increased to 10%, the ultimate strength increased to 5 ± 0.5 MPa and the modulus increased to 230 ± 30 MPa. The increase in tensile modulus may be attributed to an increase in rigidity over the pure polymer when the hydroxyapatite is added and/or the resulting strong adhesion between the two materials. The vapor phase chemical crosslinking of collagens using glutaraldehyde further increased the mechanical properties as evident from nanoindentation results. A combination of nanofibrous collagen and nanohydroxyapatite that mimics the nanoscale features of the extra cellular matrix could be promising for application as scaffolds for hard tissue regeneration, especially in low or nonload bearing areas.

Introduction

Nanostructured porous materials of biopolymers and their biocomposites that can be used as scaffolds in tissue engineering are regarded as the next frontier biomaterials in bioengineering.¹ In vitro cell seeding onto a nanostructured scaffold can allow excellent cell proliferation, migration, and differentiation of the cells into specific tissue while secreting the extra cellular matrix (ECM) components required for continuous tissue growth. The basic approach to bone tissue engineering involves the development of highly porous biodegradable 3D-scaffolds, with cells and signalling molecules, having interconnected pore network structure for cellular in-growth and facilitating nutrient and waste exchange by cells deep within the scaffolds. Many biodegradable synthetic polymers have been used in tissue engineering as 3D scaffolding materials for bone repair.^{2,3} While most conventionally fabricated scaffolds are synthetic polymer foams, the cells do not necessarily recognize these surfaces. Integrin or receptor binding is critical for the necessary cell–ECM communication that is lacking when synthetic polymers are used. The cells must attach to the scaffold to multiply, differentiate, and organize into normal healthy bone as the scaffold degrades. A well-known feature of native ECM is the nanoscaled dimensions of its

physical structure. For proper integrin binding, an ideal 3D tissue scaffold should have similarity to natural counterparts in terms of chemical composition and physical nanofibrous structure.

Electrospinning has received a great deal of attention in recent years as a method to produce the nanofibrous scaffolds for tissue engineering.^{4–12} The electrospun scaffolds have large surface area, porosity, and well interconnected pore network structure for cell adhesion and growth. Moreover, electrospun fibrous matrices with nanoscale diameters mimic morphological nanofeatures of native ECM. Electrospun nanofibers have been shown to support cell attachment and proliferation of smooth muscle cells and fibroblasts.^{13,14} Collagens are the principal structural elements of the ECM in many native tissues, and possess a nanofibrous structure with fiber bundles varying in diameter from 50 to 500 nm.¹⁵ A report on the feasibility of electrospinning of type I collagen by Matthews et al.⁶ used 1,1,1,3,3,3-hexafluoro-2-propanol (HFP) as solvent. Recently, many researchers have attempted to electrospin collagen alone or in combination with other synthetic polymers.^{16–20} Venugopal et al.¹⁶ have coelectrospun collagen and poly(caprolactone) (PCL) to obtain composite fibers and showed that the modified PCL/collagen scaffolds exhibited the required mechanical properties for the regulation of normal cell function in vascular tissue engineering. However, mechanical testing of coelectrospun nanofibrous poly(lactide-co-caprolactone) (PLCL) with type I collagen with varying collagen content from 0% to 100% (wt/wt) showed that the tensile properties decreased with increasing collagen content.¹⁹ Rho et al.¹⁸ have electrospun type I collagen using HFP as solvent into nanofibers of diameter range 100 nm to 1.2 μ m and studied the effect of collagen coating over

* To whom correspondence should be addressed. Phone: 205-975-4666. Fax: 205-934-848. E-mail: deand@uab.edu.

[†] Center for Nanoscale Materials and Biointegration (CNMB), Department of Physics.

[‡] Department of Materials Science and Engineering.

[§] Present address: Materials Science and Engineering Laboratory, National Institute of Standards and Technology (NIST), 100 Bureau Drive, Gaithersburg, MD 20899-8500.

crosslinked collagen fibers on the behavior of normal human keratinocytes in wound healing. Bone is an organic–inorganic hybrid nanobiocomposite of nanofibrous collagen and nanohydroxyapatite. On the ultrastructural level of bone, an intimate association exists between nanofibrous collagen and nanohydroxyapatite crystals (4 nm × 50 nm × 50 nm).^{21,22} Therefore, biocomposite scaffolds of nanofibrous collagen and hydroxyapatite nanoparticles could be more promising scaffolds for bone tissue engineering because of the presence of cell recognition sites in these matrices. Both the components of the nanocomposites, collagen and nanohydroxyapatite, are bioactive and osteoconductive. The present study reports the electrostatic cospinning of collagen (type I) and nanosize hydroxyapatite (nanoHA) for the first time, to our best knowledge, as potential nanofibrous osteoconductive and bioactive nanobiocomposite scaffolds.

Experimental Section

Electrospinning of Collagen and Biocomposites Fibers. Collagen type I (lyophilized sample, Sigma-Aldrich, St. Louis, MO) was dissolved in 1,1,1,3,3,3-hexafluoro-2-propanol (HFP) to obtain a viscous solution (100 mg/mL) and was electrospun at a high voltage of 25 kV (M826, Gamma High-Voltage Research, Ormond Beach FL.) to create nanofibers. The syringe was capped with an 18-gauge needle, and a feeding rate of collagen solution of 5 mL/h was set using a syringe pump (KD Scientific, Holliston, MA).⁶ A grounded aluminum collector plate was placed approximately 12.5 cm from the tip of the needle so that the electric field magnitude was 2 kV/cm. The electrospun fabrics were kept for 1 week in a vacuum desiccator to remove any residual HFP. To make composite fibers of collagen with nanoHA, nanoHA powder (Nanocerox Inc., Ann Arbor, MI) having particle size of 100–150 nm and surface area of 15 m²/g of desired amount (wt %) was well dispersed in HFP using magnetic stirring, and collagen was dissolved in it. A homogenized dispersion of collagen and nanoHA was carried out by ultrasonication for 30 min (two times) and was electrospun at a high voltage of 25 kV as described earlier. The electrospun nanobiocomposites of collagen/nanoHA were further crosslinked using 3% vapor phase glutaraldehyde in a chamber for 24 h.^{18,23} For that, the scaffolds were placed in the chamber containing a container of glutaraldehyde in a petri dish encased by Parafilm. The crosslinked collagen mats were then washed several times with phosphate buffered saline (PBS) and finally with distilled water to remove the unreacted glutaraldehyde. The crosslinked collagen mats were then dried overnight under vacuum.

Structural and Morphological Characterization. The apparent density and porosity characteristics of the electrospun scaffolds were determined as reported elsewhere²⁴ using the following equations

$$\text{apparent density (g/cm}^3\text{) of scaffold} = \frac{\text{mass of electrospun matrix (mg)}}{\text{thickness } (\mu\text{m}) \times \text{area (cm}^2\text{)}}$$

$$\text{porosity (\% of scaffold)} = \left(1 - \frac{\text{apparent density of scaffold (g/cm}^3\text{)}}{\text{bulk density of native collagen (g/cm}^3\text{)}} \right)$$

where bulk density of native collagen is 1.16 g/cm³ as reported elsewhere.^{25,26}

The morphological and structural characterizations of the electrospun composite scaffolds were carried out by scanning electron microscopy (SEM), atomic force microscopy (AFM), Fourier-transform infrared spectroscopy (FT-IR), and X-ray diffraction (XRD). Electrospun fibers were sputter coated with gold, and the morphology was observed under SEM (Philips SEM 510) at an accelerating voltage of 10 kV. SEM

Table 1. Apparent Density and Porosity Characteristics of Nanofibrous Scaffolds

no.	electrospun scaffold	apparent density (g/cm ³)	porosity (%)
1	collagen	0.0747 ± 0.002	93
2	collagen + 10% nanoHA	0.1488 ± 0.002	87
3	collagen + 20% nanoHA	0.2032 ± 0.003	82

micrographs were analyzed by an image-analyzer (Image-proplus, Media Cybernetics Co.) for the measurement of fiber diameters.

Atomic force microscopic (AFM) measurements were carried out with a Surface Probe Microscope TopoMetrix Explorer. The images were collected in contact imaging mode in ambient atmosphere. The cantilevers used were high resonance frequency (HRF) silicon nitride V-shaped cantilevers. These cantilevers end with a pyramidal tip with tip radius <50 nm and force constant of 0.032 N/m. The scanner used has a travel of 10 μm and 2 μm in the *z*-direction and 100 μm and 2 μm in the *xy*-directions. The images obtained were processed for a first-order leveling of the surface and a left shading of the image by TopoMetrix SPM Lab NT Version 5.0 software supplied with the microscope.

XRD analyses of electrospun collagen/nanoHA composites and nanoHA powders were performed on an X-ray diffractometer (Siemens D500) using Cu Kα radiation (λ = 0.1541 nm) at a current of 30 mA and an accelerating voltage of 40 kV. The spectra were recorded from 2θ = 10° to 2θ = 60° at a scanning speed of 2°/min.

Mechanical Characterization. Tensile testing and nanoindentation were used for the measurements of bulk and nanomechanical properties. The electrospun fibrous meshes were carefully cut into rectangular strips (50 mm × 6 mm). The thickness of the fibrous specimen was measured and loaded into tensile testing fixture of a dynamic mechanical analyzer (DMA, TA Instruments Inc., DE) in the ramp force mode.¹⁰ A ramp force of 0.1 N/mm was applied. The displacement was measured with an optical encoder. The stress versus strain curves were generated for different samples (*n* = 5) and used to determine the modulus and strength values. The data were reported as mean ± standard deviation.

Nanomechanical properties of the nanofibrous composite scaffolds of collagen/nanoHA were carried out by nanoindentation using a Nanoindenter XP (MTS Systems, Oak Ridge, TN) system.¹¹ The system was calibrated by using silica samples for a range of operating conditions. Young's modulus and hardness of silica were calculated respectively as 70 and 9.1 GPa. The tests were run at a constant strain rate of 0.05 s⁻¹ using a continuous stiffness measurement (CSM) option. As the nanoindenter tip approached the maximum penetration depth, the load was held constant for 10 s to stabilize the creep found in the material. For all the measurements, a maximum depth of 500 nm was given. A Berkovich diamond indenter with total included angle of 142.3° was used for nanoindentation measurements. Before doing indentation on the sample, indenter to microscope calibration was done in order to locate the indentation site properly for each sample. The data were processed using proprietary software provided by MTS (TestWorks 4, MTS Systems, Oak Ridge TN) to produce load-displacement curves, and the mechanical properties were calculated using the Oliver and Pharr method.²⁷

Results and Discussion

The complex hierarchical nanostructure of natural bone having hydroxyapatite, the major mineral phase, and collagen has motivated the idea of coelectrospinning of nanobiocomposite fibers of collagen and nanohydroxyapatite. Type I collagen was coelectrospun with nanoHA to obtain bioactive nanocomposite scaffolds with filler content from 0 to 20 wt % to mimic the physical nanofeatures and composition of bone. Higher percentage loading of nanoHA resulted with an agglomeration and poor dispersion of nanoHA particles due to their comparatively larger particle size (100–150 nm). The structure and morphology of

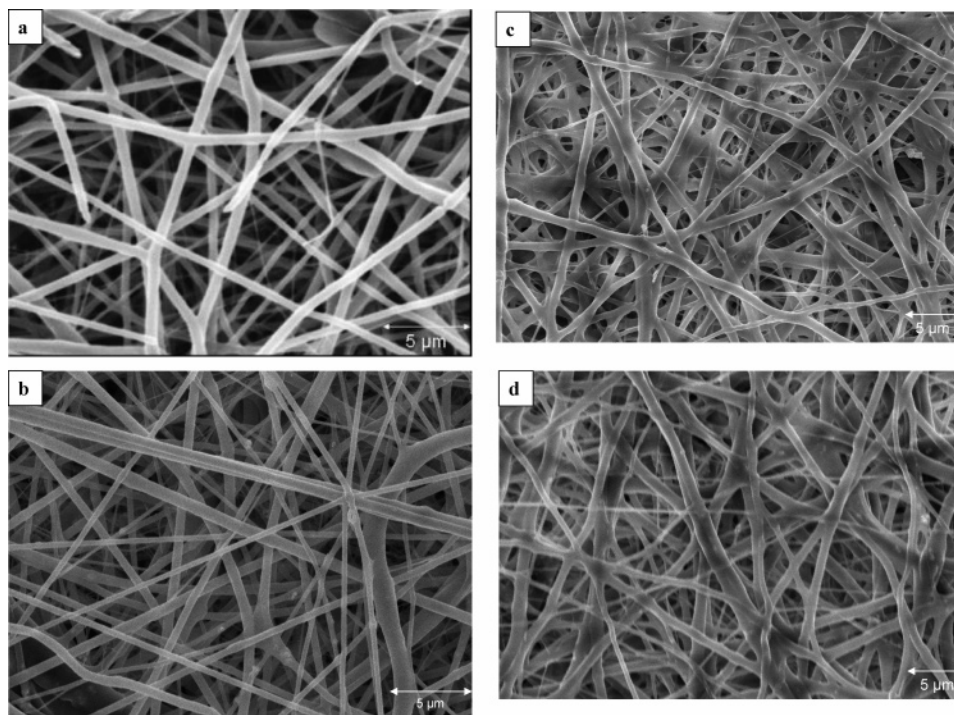


Figure 1. SEM micrographs of electrospun scaffolds: (a) collagen fibers, (b) collagen + 10% nanoHA (uncrosslinked), (c) collagen + 10% nanoHA (crosslinked), and (d) collagen + 20%HA (crosslinked). Scaffolds become dense due to chemical crosslinking.

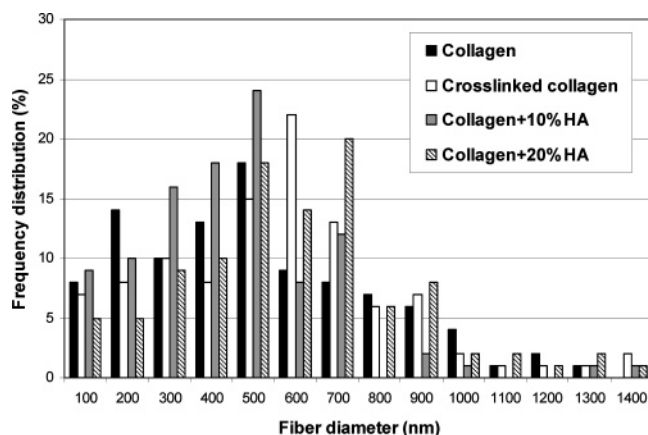


Figure 2. Frequency distribution of fiber diameters of nanofibrous scaffolds. As the nanoHA content increases, the distribution maximum shifts to higher diameter region.

nanocomposite fibrous matrices are shown in the SEM micrographs (Figure 1a–d). The electrospun nanocomposite fibers on the collector formed a randomly oriented nonwoven fabric structure having nanofibers in the 500–700 nm diameter range, depending on the composition and crosslinking. The present nanofibrous biocomposite scaffolds have well interconnected pore network structure and large surface area necessary for cellular attachment, vascularization, and resulting cellular in-growth. The porosity calculation from apparent density measurements of the matrices showed 93–82% porosity, depending on the nanoHA loading in electrospun collagens (Table 1). The SEM images showed that electrospun fabrics of both collagen and biocomposites obtained were devoid of any beads under the optimized spinning conditions (electric potential = 25 kV, flow rate = 5 mL/h, collagen concentration in HFP = 10% (wt/v), and distance between needle and collector = 12.5 cm). Figure 2 indicates the frequency distribution of fiber diameters of electrospun pure collagen, collagen + 10% nanoHA, and collagen + 20% nanoHA. In natural tissues, the collagen fibers

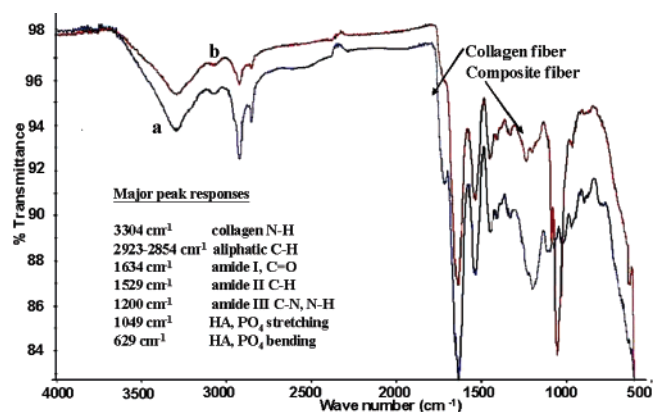


Figure 3. ATR-FTIR spectra of collagen and collagen + 20% nanoHA composite scaffolds. Peaks around 1049 and 629 cm⁻¹ in composite spectrum are due to the presence of HA particles in the fibers.

have diameters in the range from 50 to 500 nm.¹⁵ The present collagen/nanoHA composite scaffolds have a majority of the fibers in the upper range of nanoscale features of the natural ECM. Interestingly, the majority of the fibers of electrospun collagen (pure) have fiber diameter in the range from 100 to 500 nm. As the loading of nanoHA in fibers increased to 20%, the distribution maximum shifts to higher diameter region for collagen + 20% nanoHA composite fibers. This indicates that the diameter of composite fibers increases with increase of nanoHA content. With higher nanoHA content (20 wt %), the effect of concentration (viscosity) on fiber diameter plays a role and results in a broader diameter distribution. The vapor phase crosslinking of collagen using glutaraldehyde has not affected the morphology of fibrous matrices as evident from the SEM micrographs of crosslinked scaffolds (Figure 1c,d). The crosslinked collagen scaffolds exhibited a higher dimensional stability in aqueous medium due to chemical crosslinking as reported elsewhere.¹⁸

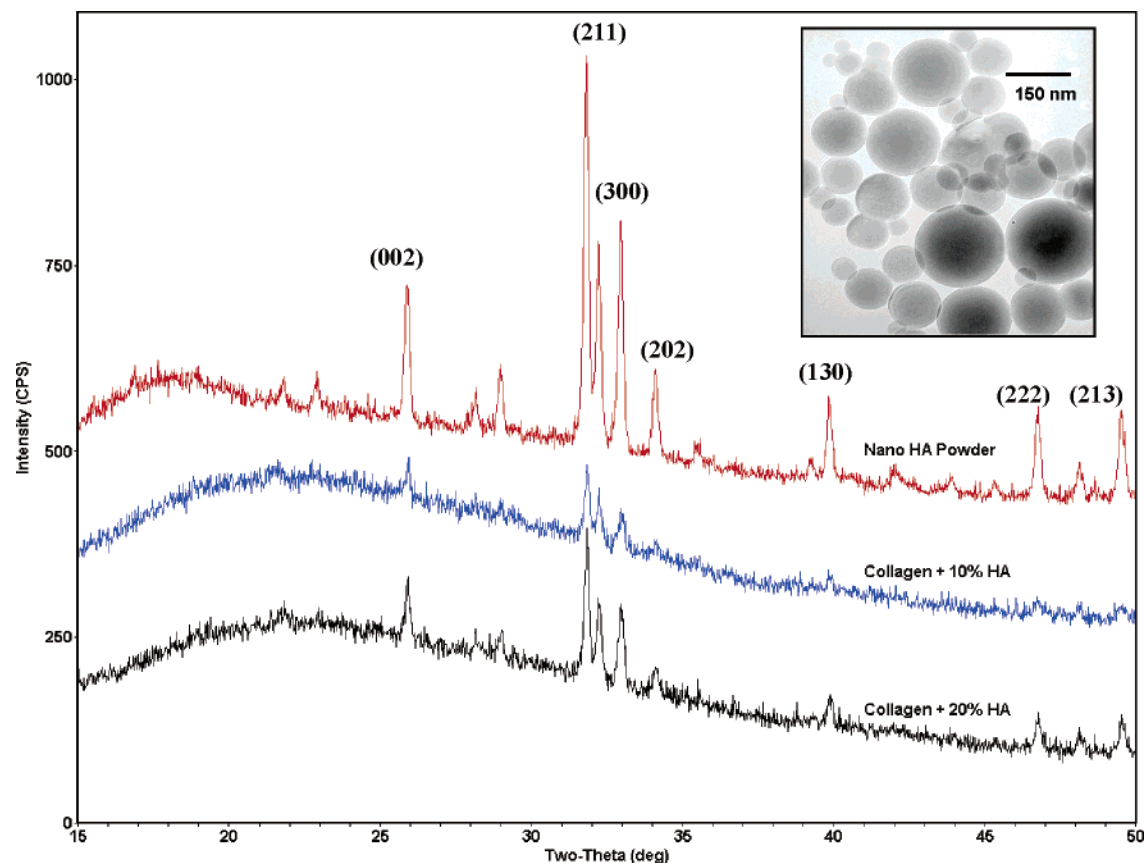


Figure 4. XRD spectra of nanoHA powder and collagen/nanoHA biocomposite scaffolds. Inset: TEM image of nanoHA powders. Intensity of the HA peaks in biocomposite spectra increases with increase of nanoHA content.

The presence of nanoHA in the fibers was confirmed by FT-IR, and XRD spectra of collagen/nanoHA composites. The FT-IR spectrum (Figure 3) of the electrospun collagen/nanoHA composite fibers showed characteristic peaks for collagen and hydroxyapatite. The amide I peak at 1633 cm^{-1} (C=O stretching), amide II peak at 1529 cm^{-1} (N-H deformation), and amide III peak around 1200 cm^{-1} (N-H deformation) in collagen and collagen/nanoHA biocomposite were observed. The amide I, II, and III band regions of collagen are directly related to polypeptide conformation. The amide I band with characteristic frequencies in the range from 1600 to 1700 cm^{-1} is mainly associated with the stretching vibrations on carbonyl groups along the polypeptide backbone and is a sensitive marker of polypeptide secondary structure.^{28,29} There are C-N stretching vibrations and N-H bending vibrations as minor vibration modes of amide II and amide III bands. The typical bands such as N-H stretching at 3303 cm^{-1} for amide A and C-H stretching at 3068 cm^{-1} for amide B were also found in both collagen and collagen biocomposite with nanoHA. The characteristic peaks for nanoHA are clearly present in the collagen/nanoHA biocomposite spectrum (Figure 3b). The PO_4^{3-} stretching band around 1080 cm^{-1} and (P-O) of PO_4^{3-} bending bands in the $570\text{--}610\text{ cm}^{-1}$ range are due to the presence of nanoHA. The carbonyl peaks for -COOH end groups of collagen found at 1716 cm^{-1} in the collagen spectrum disappeared or became minimal in the biocomposite spectrum. This can be attributed to a weak interaction (ion-dipole bond) of the polar carboxylic group with Ca^{2+} ions of hydroxyapatite due to salt formation. Because of these weak bond formations, the nanosized HA particles could be well dispersed in collagen matrix. In addition, the aliphatic C-H band of collagen around $2800\text{--}2900\text{ cm}^{-1}$ and hydrogen-bonded N-H around 3500 cm^{-1} were also present in both collagen and the composite spectra.

The reflection planes corresponding to the characteristic XRD spectral peaks of nanoHA based nanobiocomposite scaffolds are given in Figure 4. The peak maxima at 25.9° , 31.69° , 32.18° , 32.79° , 34.03° , 46.60° , and 49.46° in the diffraction patterns of collagen/nanoHA composites are, respectively, due to hydroxyapatite *d*-spacing of 3.44 , 2.8237 , 2.7821 , 2.7309 , 2.6343 , 1.9489 , and 1.8429 \AA . Inset in Figure 4 is a TEM image of the nanoHA showing a particle size of $100\text{--}150\text{ nm}$. The presence of hydroxyapatite particles in individual fibers was further confirmed by contact mode AFM imaging. Figure 5 shows the AFM images of pure collagen and collagen + 20% nanoHA composite fibers. The minerals are distributed in the collagen fiber matrix. Due to the addition of nanoHA, the surface roughness of the collagen fibers increases as evident from AFM images (Figure 5). The electrospun nanobiocomposite of collagen and nanoHA not only mimics the chemistry but also has the micro/nanostructure of the natural bone to some extent.

It is known that mechanical properties of the ECM environment can influence intracellular signaling and cell response.³⁰ Cell adhesion to scaffold substrates in molecular pathways is controlled by adhesion complexes and the actin/myosin cytoskeletons. The local nanomechanical properties of scaffolds in contact with cytoskeleton likely have important implications for cell differentiation and regenerative functions.³¹ Figure 6 shows the nanoindentation load-displacement curves of electrospun pure collagen and collagen/nanoHA composite fibers (uncrosslinked) with various nanoHA filler content. For a constant indentation depth of 500 nm , the maximum load (P_{max}) for electrospun collagen increases with increasing loading of nanoHA in fiber. The effect of nanoHA content on the mechanical properties of fibers is given in Figures 7 and 8. The hardness and Young's modulus of the electrospun collagen/nanoHA composite fibers increase with the increase of nanoHA

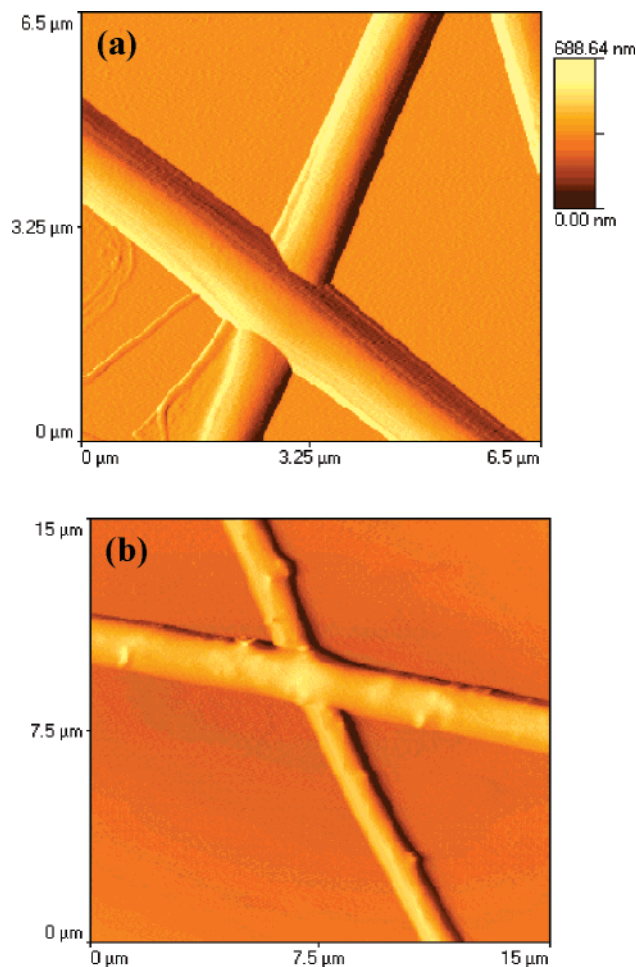


Figure 5. Contact mode AFM images of electrospun fibers on mica: (a) collagen, and (b) collagen + 20% nanoHA composite. Surface roughness of the electrospun fibers increases with the presence of nanoHA.

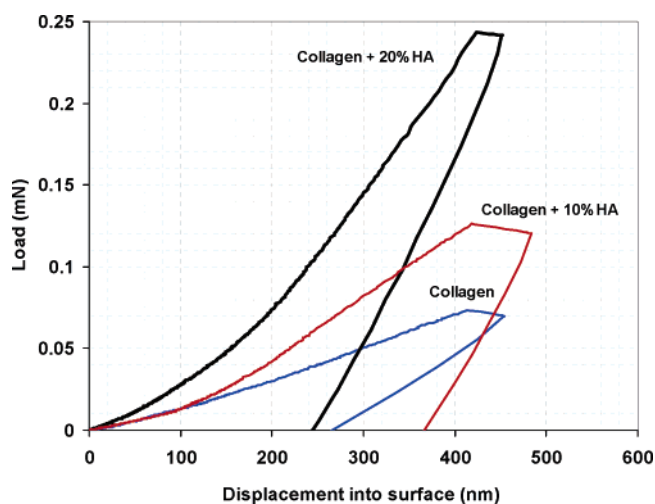


Figure 6. Nanoindentation load-displacement curves of collagen/nanoHA biocomposites. As nanoHA content in the fiber increases, the maximum load also increases.

content. The collagen + 20% nanoHA composite fiber showed a 3-fold increase in Young's modulus compared to that of pure collagen (uncrosslinked) fiber (Figure 7). The glutaraldehyde crosslinking of collagen was further found to have a marked effect on the Young's modulus (Figure 7) and the hardness (Figure 8) of the composite fibers. The Young's modulus values were found to be almost doubled in the case of crosslinked

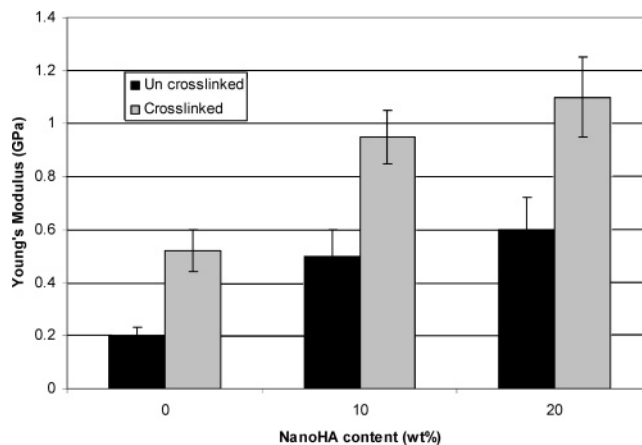


Figure 7. Effect of nanoHA content on Young's modulus of collagen/nanoHA biocomposite fibers. The Young's modulus increases with increase in nanoHA content and also with crosslinking of collagen.

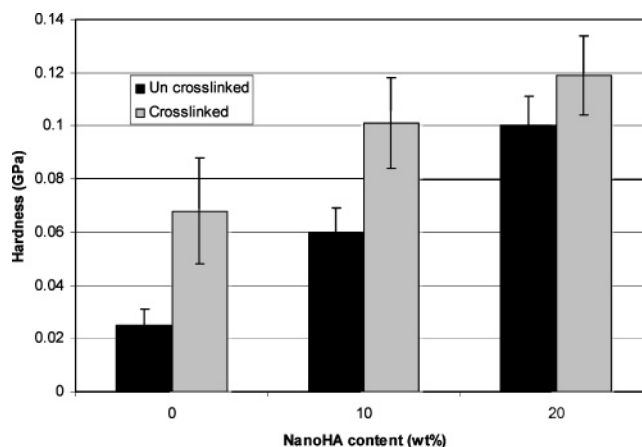


Figure 8. Effect of nanoHA content on hardness of collagen/nanoHA biocomposite fibers. The hardness of fibers increases with addition of nanoHA and also with crosslinking of collagen.

collagen and crosslinked collagen/nanoHA composite fibers in comparison with uncrosslinked fibers. This is due to interchain crosslinking of collagen molecules, resulting in increased stiffness of fibers.

Nanomechanical properties of electrospun fibers, measured at a small length scale, may differ from bulk mechanical properties (tensile) of the electrospun scaffolds at macroscale.¹¹ This is because the tensile properties of the porous electrospun materials, in bulk, mainly depend on their porosity, total fiber content, and orientation of fibers with respect to the direction of application of tensile force. Therefore, electrospun meshes showed lower tensile properties than thin films or sheets. The tensile properties of electrospun pure collagen and collagen/nanoHA composite meshes (uncrosslinked) are shown in Figure 9. The pure collagen fibrous matrix (without nanoHA) showed an average tensile strength of 1.68 ± 0.10 MPa and modulus of 6.21 ± 0.8 MPa with an average strain value of $55 \pm 10\%$. The results were in agreement with the tensile strength of electrospun type I collagen mat onto a rectangular target mandrel rotating at 4500 rpm (with a linear velocity of 1.4 m/s) reported by Matthews et al.⁶ The scaffolds cut in parallel with the principal axis fibril alignment, in their report, indicated an average peak stress of 1.5 ± 0.2 MPa.⁶ However, dispersion of nanoHA particles in polycaprolactone fibers increased the mechanical properties of electrospun scaffolds as reported elsewhere.¹⁰ This indicates that nanocomposite fibers have better mechanical properties than pure polymer fibers. The collagen/

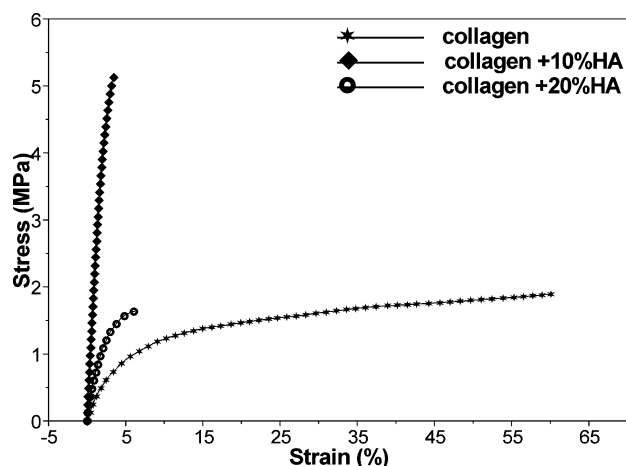


Figure 9. Tensile properties of collagen and collagen/nanoHA biocomposite scaffolds (uncrosslinked). With the addition of nanoHA, the collagen scaffolds become more brittle in nature.

nanoHA nanocomposite meshes also showed higher tensile properties than pure collagen mesh. As the nanoHA content in the collagen nanofibers increased to 10%, the ultimate strength increased to 5 ± 0.5 MPa and the modulus increased to 230 ± 30 MPa, with a drastic decrease of strain to 3%. The increase in tensile modulus may be attributed to an increase in rigidity over the pure polymer when the hydroxyapatite is added and/or to the resulting strong adhesion between the two materials. At lower wt % loading, the collagen–HA interface interaction could have resulted from the homogeneous dispersion of nanoHA, which in turn could be due to the interaction between the calcium ions of HA with the carboxyl groups of the collagen molecules. However, further increase in nanoHA content decreased the tensile properties of nanocomposite scaffolds as reported by Fujihara et al.³² Collagen + 20% nanoHA composite scaffold showed an average ultimate strength of 2.2 ± 0.15 MPa (Figure 9). The composite scaffolds were found to be brittle in nature. Higher percentage loading of nanoHA might have resulted in poor interface bonding of the nanoHA powder with collagen and/or a decrease in chain entanglements in polymer, which would be reflected in tensile properties. The tensile testing of chemically crosslinked collagen matrices was unsuccessful due to their highly brittle nature. The crosslinked materials were found to be too brittle to even fix the specimen between the grips of the test machine. However, nanoindentation results, for a constant depth of 500 nm, showed higher modulus for crosslinked samples than for the uncrosslinked ones.

The ultimate tensile strength of uniaxially tested natural articular cartilage tissues ranges from 9 to 18 MPa, with an ultimate strain of 15–120%.³³ Mechanical property measurements at macro and nano levels showed that the electrospun biocomposite scaffolds of collagen/nanoHA were stiff, but were not able to attain high tensile strength, which may be due to lack of hydration and other native matrix constituents in the scaffolds. However, mechanomorphological properties suggest that an electrospun biocomposite scaffold of collagen/nanoHA may be a potential candidate material for use in bone tissue engineering of low and/or nonload bearing areas. It has also been reported that chondrocyte adhesion and proliferation on polymer/nanoHA composite materials are better than for the pure polymer.³⁴ Nanosized HA, compared to microsized HA, can promote cell adhesion, differentiation, and proliferation, osteointegration, and deposition of calcium mineral of the surface which in turn leads to enhanced formation of new bone tissue within a short duration.³⁵ Nanofibrous scaffolds of PCL

have shown favorable cell adhesion and spreading of human mesenchymal stem cells (hMSCs) in vitro.⁴ The osteoconductive and osteoinductive collagenous nanofibrous scaffolds having nanoHA may be more capable of initiating the de novo bone formation in vivo.

Conclusion

Nanostructured biocomposite scaffolds of type I collagen and nanohydroxyapatite of varying compositions (wt %) were prepared by electrostatic co-spinning. FTIR, AFM, and XRD techniques used for structural characterization confirmed the presence of well-dispersed nanoHA mineral phase in the collagen matrix. The porosity calculation from apparent density measurements showed 82–93% porosity for the present electrospun biocomposite scaffolds. SEM analyses showed a well-interconnected pore network structure with nanofibrous morphology of randomly oriented fibers in the diameter range 500–700 nm, depending on the composition. The fiber diameter increased with an increase in nanoHA content. AFM analyses of single fiber showed increased surface roughness of composite fibers compared to neat collagen fibers. Tensile testing (macroscale) and nanoindentation (nanoscale) were used for the mechanical characterization. Nanomechanical properties of individual electrospun fibers, measured at small length scale, differ significantly from bulk mechanical properties (tensile) of the electrospun scaffolds at macroscale. The pure collagen fibrous matrix (without nanoHA) showed an average tensile strength of 1.68 ± 0.10 MPa and modulus of 6.21 ± 0.8 MPa with an average strain value of $55 \pm 10\%$. As the nanoHA content in the nanofibers increased to 10%, the ultimate strength increased to 5 ± 0.5 MPa and modulus to 230 ± 30 MPa. The increase in tensile modulus may be attributed to an increase in rigidity over the pure polymer when the hydroxyapatite is added and/or the resulting strong adhesion between the two materials. The chemical crosslinking of collagen using glutaraldehyde further increased the mechanical properties as evident from nanoindentation results. In conclusion, a combination of nanofibrous collagen and nanohydroxyapatite (nanoHA) that mimics the nanoscale features of extra cellular matrix could be promising scaffolding materials for bone tissue regeneration in nonload bearing applications.

Acknowledgment. The authors acknowledge the support from the National Science Foundation (NSF)-Nanoscale Interdisciplinary Research Team (NIRT) award under Grant DMR-0402891. We also acknowledge partial support from the UAB Center for Metabolic Bone Disease (CMBD) and UAB Center for Nanoscale Materials and Biointegration (CNMB). Thanks are also due to Dr. Jonathan F. Sullivan for acquiring the XRD spectra and to Mr. Sharon Paras, Nanocerox Inc., for the TEM image of nanohydroxyapatite.

References and Notes

- (1) Wen, X.; Shi, D.; Zhang, N. Applications of Nanotechnology in Tissue Engineering. In *Handbook of Nanostructured Biomaterials and Their Applications in Nanobiotechnology*; Nalwa, H. S., Ed.; American Scientific Publishers: California, 2005; Vol. 1, pp 1–23.
- (2) Agarwal, C. M.; Ray, R. B. *J. Biomed. Mater. Res.* **2001**, *55*, 141.
- (3) Thomson, R. C.; Wake, M. C.; Yaszemski, M. J.; Mikos, A. G. *Adv. Polym. Sci.* **1995**, *122*, 245.
- (4) Yoshimoto, H.; Shin, Y. M.; Terai, H.; Vacanti, J. P. *Biomaterials* **2003**, *24*, 2077.
- (5) Li, W. J.; Laurencin, C. T.; Caterson, E. J.; Tuan, R. S.; Ko, F. K. *J. Biomed. Mater. Res.* **2002**, *60*, 613.
- (6) Matthews, J. A.; Wnek, G. E.; Simpson, D. G.; Bowlin, G. L. *Biomacromolecules* **2002**, *3*, 232.

- (7) Xu, C. Y.; Inai, R.; Kotaki, M.; Ramakrishna, S. *Tissue Eng.* **2004**, *10*, 1160.
- (8) Zong, X.; Bien, H.; Chung, C. Y.; Yin, L.; Fang, D.; Hsiao, B. S.; Chu, B.; Entcheva, E. *Biomaterials* **2005**, *26*, 5330.
- (9) Khil, M. S.; Bhattarai, S. R.; Kim, H. Y.; Kim, S. Z.; Lee, K. H. *J. Biomed. Mater. Res.: Appl. Biomater.* **2005**, *72*, 117.
- (10) Vinoy Thomas; Jagani, S.; Johnson K; Jose, M. V.; Dean, D. R.; Vohra, Y. K.; Nyairo E. *J. Nanosci. Nanotechnol.* **2006**, *6*, 487.
- (11) Vinoy Thomas; Jose, M. V.; Chowdhury, S.; Sullivan, J. F.; Dean, D. R.; Vohra, Y. K. *J. Biomater. Sci., Polym. Ed.* **2006**, *17*, 969.
- (12) Tan, S. R.; Inai, R.; Kotaki, M.; Ramakrishna, S. *Polymer* **2005**, *46*, 6128.
- (13) el-Kenawy, R.; Layman, J. M.; Watkins, J. R.; Bowlin, G. L.; Matthews, J. A.; Simpson, D. G.; Wnek, G. E. *Biomaterials* **2003**, *24*, 907.
- (14) Xu, C. Y.; Inai, R.; Kotaki, M.; Ramakrishna, S. *Biomaterials* **2004**, *25*, 877.
- (15) Elsdale, T.; Bard, J. *J. Cell Biol.* **1972**, *54*, 626.
- (16) Venugopal, J.; Zhang, Y. Z.; Ramakrishna, S. *Nanotechnology* **2005**, *16*, 2138–2142.
- (17) Buttafoco, L.; Kolkman, N. G.; Engbers-Buijtenhuijs, P.; Poot, A. A.; Dijkstra, P. J.; Vermes, I.; Feijen, J. *Biomaterials* **2006**, *27*, 724.
- (18) Rho, K. S.; Jeong, L.; Lee, G.; Seo, B. M.; Park, Y. J.; Hong, S. D.; Roh, S.; Cho, J. J.; Park, W. H.; Min, B. M. *Biomaterials* **2006**, *27*, 1452.
- (19) Kwon, K.; Matsuda, T. *Biomacromolecules* **2005**, *6*, 2096.
- (20) Telemeco, T. A.; Ayres, C.; Bowlin, G. L.; Wnek, G. E.; Boland, E. D.; Cohen, N.; Baumgarten, C. M.; Mathews, J.; Simpson, D. G. *Acta Biomater.* **2005**, *1*, 377.
- (21) Rho, J.; Kuhn-Spearing, L.; Zioupos, P. *Med. Eng. Phys.* **1998**, *20*, 92.
- (22) McConnell, D. *Clin. Orthop. Relat. Res.* **1962**, *23*, 253.
- (23) Shields, K. J.; Beckman, M. J.; Bowlin, G. L.; Wayne, J. *Tissue Eng.* **2004**, *10*, 1510.
- (24) He, W.; Yong, T.; Teo, W. E.; Ma, Z.; Ramakrishna, S. *Tissue Eng.* **2005**, *11*, 1574.
- (25) Hulmes, D. J. S.; Miller, A.; White, S.; Doyle, B. B. *J. Mol. Biol.* **1977**, *110*, 643.
- (26) Dweltz, N. E. In *Collagen*; Ramanathan, N., Ed.; Interscience: New York, 1962; p 179.
- (27) Oliver, W. C.; Pharr, G. M. *J. Mater. Res.* **1992**, *7*, 1564.
- (28) Doyle, B. B. *Biopolymers* **1975**, *14*, 937.
- (29) Payne, K. J.; Veis, A. *Biopolymers* **1991**, *30*, 2372.
- (30) Geiger, B.; Bershadsky, A.; Pankov, R.; Yamada, K. M. *Nat. Rev. Mol. Cell Biol.* **2001**, *2*, 793.
- (31) Discher, D. E.; Janmey, P.; Wang, Y. *Science* **2005**, *310*, 1139.
- (32) Fujihara, K.; Kotaki, M.; Ramakrishna, S. *Biomaterials* **2005**, *26*, 4139.
- (33) Woo, S.; Buckwalter, J. In *American Academy of Orthopedic Surgeons Symposium*; Woo, S., Buckwalter, J., Eds.; Savannah, Georgia, 1988, p 401.
- (34) Hong, Z.; Zhang, P.; He, C.; Qiu, X.; Liu, A.; Chen, L.; Chen, X.; Jing, X. *Biomaterials* **2005**, *26*, 6296.
- (35) Webster, T. J.; Siegel, R. W.; Bizios, R. *Biomaterials* **2000**, *21*, 1803.

BM060879W